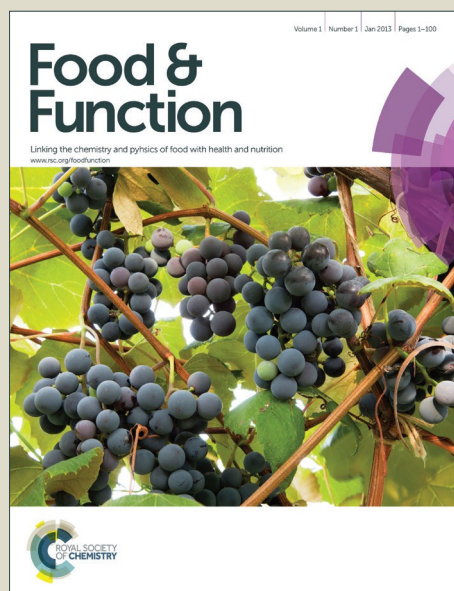


Food & Function

Accepted Manuscript



This is an *Accepted Manuscript*, which has been through the Royal Society of Chemistry peer review process and has been accepted for publication.

Accepted Manuscripts are published online shortly after acceptance, before technical editing, formatting and proof reading. Using this free service, authors can make their results available to the community, in citable form, before we publish the edited article. We will replace this *Accepted Manuscript* with the edited and formatted *Advance Article* as soon as it is available.

You can find more information about *Accepted Manuscripts* in the [Information for Authors](#).

Please note that technical editing may introduce minor changes to the text and/or graphics, which may alter content. The journal's standard [Terms & Conditions](#) and the [Ethical guidelines](#) still apply. In no event shall the Royal Society of Chemistry be held responsible for any errors or omissions in this *Accepted Manuscript* or any consequences arising from the use of any information it contains.

Structural stability and Sin a 1 anti-epitope antibody binding ability of yellow mustard (*Sinapis alba* L.) napin during industrial-scale myrosinase inactivation process

Harsha K. Marambe^{1,2}, Tara C. McIntosh¹, Bifang Cheng¹, Janitha P.D. Wanasundara^{1*}

¹Agriculture and Agri-Food Canada, Saskatoon Research Centre
107 Science Place, Saskatoon SK S7N 0X2 Canada

²Present address: Prairie Tide Chemicals Inc., 102 Melville Street
Saskatoon SK S7J 0R1 Canada

*Corresponding author address:

Agriculture and Agri-Food Canada, Saskatoon Research Centre
107 Science Place, Saskatoon SK S7N 0X2 Canada
Janitha.wanasundara@agr.gc.ca
Tel: +1 306 385 9455

Abstract

This study investigated the structural stability of yellow mustard (YM, *Sinapis alba* L.) napin and the changes of its Sin a 1 anti-epitope antibody binding ability during myrosinase enzyme inactivation process. Food industry uses myrosinase inactivated, non-pungent YM for the uses beyond spice applications. Napin was isolated from seeds received from an industrial processor before (YM+M) and after (YM-M) myrosinase inactivation. Thermal stability, secondary and tertiary structure features and surface hydrophobicity parameters of napin were analyzed. The Sin a 1 content in YM seeds and the stability of Sin a 1-containing napin during simulated *in vitro* gastrointestinal (GI) digestion were determined by non-competitive indirect enzyme linked immunosorbent assay using the Sin a 1 anti-epitope antibody (AE-Ab) as the primary Ab. YM napin retained the dominant alpha-helical components of secondary structure and the tertiary structure folds during this process. Napin of YM-M showed changes in hydrophobicity parameters of the molecules and binding ability of AE-Ab; 2.19 ± 0.48 g/100 g of YM-M seeds vs 1.49 ± 0.16 g/100 g YM+M seeds. Proteins of YM-M was more susceptible for *in vitro* GI digestion and also showed reduction in AE-Ab reactivity upon digestion; 1.81 ± 0.07 mg/g of YM+M vs 1.71 ± 0.15 mg/g of YM-M seeds. This suggests that the myrosinase inactivation process has induced surface modification of napin exposing Sin a 1 epitope leading to an increase in AE-Ab binding. However, the epitope region of YM-M napin showed improved susceptibility for hydrolysis during GI digestion resulting in less number of available epitope regions suggesting possible reduction in napin immune reactivity.

Keywords

napin, mustard allergens, 2S structure, myrosinase inactivation, digestibility, yellow mustard

Introduction

Mustard seed has the characteristic, intense hot flavor or pungency, which is vital for its use as a spice and condiment. Yellow mustard (YM; *Sinapis alba* L.) predominantly contains sinalbin or benzyl glucosinolate and the endogenous enzyme myrosinase catalyses the hydrolysis of sinalbin to generate 4-hydroxy benzyl isothiocyanate (p-HBIT), which gives the sharp pungency^{1,2}. The heat sensation caused by p-HBIT in mouth can overpower the other food flavors and considered a limitation to use YM other than a spice^{3,4}. Besides the glucosinolates, YM seed is rich in oil (~30%) and protein (~30%) in the cotyledons and also soluble polysaccharides (~5%) located primarily in the seed coat⁵. Seed coat polysaccharides (mucilage or gums) together with cotyledon proteins give rheological properties similar to many other hydrocolloids making YM flour a very attractive techno-functional ingredient for food products. However, arresting pungency generation is necessary when YM is in high inclusion levels and it can be achieved by inactivating endogenous myrosinase. Thermal treatment of YM with active, endogenous myrosinase (YM+M) deactivates the enzyme and produces “deheated” or less-pungent YM (YM-M), in which sinalbin remains intact without formation of p-HBTC because of the denaturation of endogenous catalyst for sinalbin hydrolysis. The YM-M has no pungency, but retains the complete spectrum of functional properties that are characteristic of mustard flour. Currently, YM-M is a protein-rich food ingredient with binder-extender and viscosity and texture enhancer capabilities in cooked meat products, sauces and ketchup without any flavor impact⁴. Meat industry uses YM-M as an emulsifier, water binder and a bulking agent¹. Besides protein and polysaccharide gums, YM seed is an inexpensive source of natural antioxidants⁶ and the strong antioxidant activity of YM extracts against meat lipid oxidation are retained during this enzyme inactivation process⁷.

Some proteins of mustard are gastro-intestinal (GI) allergens making mustard as a priority food allergen source in EU and Canada. In YM, Sin a 1 (a 2S napin), Sin a 2 (a 11S cruciferin) Sin a 3 (a lipid transfer protein; LTP) and Sin a 4 (a profilin) are identified and characterized as allergens that can lead to IgE mediated allergic reactions. Of these, Sin a 1 is the major YM allergen and considered as the most suitable diagnostic marker to determine genuine sensitization to mustard⁸. Sin a 1 is characterized as a compact Glu-rich, basic (isoelectric pH=11), low molecular weight (14.1 kDa) protein composed of two disulfide bonded polypeptides; a small

(39 amino acids) and a large (88 amino acids) subunit (Fig. 1)^{9,10}. Five α -helices (Ia, Ib, II, III and IV) of these two peptides are bundled and form the three dimensional structure typical to napin (Fig. 1). Epitope mapping studies of Sin a 1 were able to locate a linear epitope in the hypervariable region, which is the short segment that connects α -helices III and IV (Fig. 1)^{11,12}. In a recent study, we analyzed the Sin a 1 content of four commercial YM varieties of Canada using Sin a 1 anti-epitope antibody (AE-Ab) based non-competitive indirect enzyme linked immunosorbent assay (NCI-ELISA) and the levels were between 2.6 and 5.9 g/100 g seeds, which was less than the total napin content (4.3 to 9.2 g/100 g seeds), suggesting that YM napin is a mixture of homologous proteins in which Sin a 1 is a component¹³.

Structural aspects of allergenic proteins, especially the solubility, stability, size, and compactness of the overall folds play a critical role in its immunochemical properties. The protein structure determines the surface exposure of epitopes for IgE recognition and the structural alterations such as unfolding and fragmentation can change the IgE binding capability of the molecule therefore the allergenicity. The structural features of allergen molecules make them stable and less prone to hydrolysis by digestive tract proteases thus increasing the availability for antibody binding¹⁴. The 2S albumins of seeds are considered stable for thermal and proteolytic cleavage due to their disulfide bonding pattern and electrostatic interactions, therefore becomes molecules that are highly probable to reach intestinal mucosa in intact form for absorption¹⁵. Similarly, Sin a 1 is characterized as a thermo stable protein that is resistant to digestion by trypsin and other proteolytic enzymes¹⁶. Currently, information on industrial-scale myrosinase inactivation process on physicochemical and allergenic properties of Sin a 1 or napin is not available. The aim of this study was to investigate the impact of myrosinase inactivation process on the structural and *in vitro* digestive properties and Sin a 1 anti-epitope antibody (Sin a 1 AE-Ab) binding ability of YM napin that contains Sin a 1.

Experimental

Materials

Samples of YM seed before going through myrosinase inactivation process (YM+M) and after inactivation of myrosinase (YM-M) was obtained from an industrial-scale dry mustard processing facility (GS Dunn limited, Hamilton Ontario, Canada). Seed samples were withdrawn

from three different occasions within a 3-month period. The Sin a 1 epitope peptide synthesis and generation of Sin a 1 AE-Ab was similar to Marambe *et al.*¹³ The BCA assay kit was purchased from Pierce Thermochemical, USA. All the other chemicals used were from Sigma, Co. Canada and were of reagent grade.

Experiments

Napin extraction and purification

First, whole YM seeds were ground to a coarse powder using a home-style coffee grinder and then defatted with n-hexanes using the swedish tube method¹⁷. Defatted YM (50 g) was mixed with deionized water (meal:water 1:13.5, w:v) and CaCl₂ (final concentration of 0.15 M) and the slurry pH was adjusted to 3.0 using 1 M H₂SO₄. After vigorous stirring for 1 h at 30 °C, the slurry was centrifuged (2000×g) for 10 min at 20°C and the supernatant was recovered and filtered under vacuum using Whatman #1 filter paper. The residual meal was re-extracted with 350 mL of deionized water using same conditions as mentioned above. The pooled supernatant was adjusted to pH 7 using 10 M NaOH and the solution was centrifuged to remove any precipitate. The supernatant was diafiltered using Pellicon-2 tangential flow filtration system (MWCO: 5 kDa) to remove salts and other low molecular weight substances. The retentate containing desalted napin was freeze dried and stored at -20°C until use¹⁸.

Preparation of napin standard for ELISA

The dry napin obtained from defatted YM (variety: Andante) meal was dissolved in buffer A (50 mM Tris HCl+ 5mM EDTA+0.3% NaHSO₃; pH: 8.5; 50 mg/mL) and injected to a cation exchange column (CEC, Resource S, injection volume 17 mL; Flow rate: 1.5 mL/min) connected to AKTA-FPLC system. Napin bound to the column material was eluted using a salt gradient (0-50%) with buffer B (50 mM Tris-HCl+1M NaCl+5mM EDTA+0.3% NaHSO₃; pH: 8.5). Eluted napin in buffer B was desalted using a desalting column (Hi-Prep 26/10; injection volume: 12 mL) with deionized water as mobile phase at a flow rate of 3 mL/min and freeze dried to use as the standard for ELISA.

Analysis of protein content

The total protein content of YM seeds, napin and chromatographically purified napin standard was determined by combustion N analysis using a Thermo Erba N analyzer and EDTA as the standard. The N values were converted to protein by multiplying with a conversion factor (6.25). The protein contents of the reconstituted napin solutions were analyzed using Bicinchoninic acid assay (BCA assay) using bovine serum albumin (BSA) as the standard¹⁹.

Circular Dichroism (CD)

The secondary and tertiary structures of napin extracted from YM+M and YM-M were assessed by obtaining the CD spectra in the far UV (180-260 nm) and near UV (260-320 nm) regions, respectively. The stock solutions of napin were filtered (0.45 µm syringe filters) and diluted with degassed and filtered superQ water to achieve an appropriate protein concentration that yielded an absorbance value < 1 in the respective wavelength range. The CD spectra were obtained using a Pistar-180 spectrometer purged with N₂ gas at 25°C. The far UV-CD spectra were recorded using a quartz demountable cell (Hellma Analytics; path length: 0.01 cm) and the near UV-CD spectra were recorded using a quartz cell of 1 cm path length (Hellma Analytics). The instrument was calibrated daily with camphor sulfonic acid (CSA) prior to taking measurements. The CD spectra of each napin solution was obtained in duplicate and averaged. A CD spectrum of appropriate blank was obtained in duplicate, averaged and subtracted from each sample spectra prior to data analysis. The secondary structure composition of protein samples was obtained by analyzing far UV-CD spectra using the CDNN software. Deconvolution of 13, 23 and 33 base spectra was assessed to obtain the best deconvolution that yielded the total secondary structure content in 180 to 260 nm more similar to 100%.

Surface hydrophobicity parameters

The fluorescent probe, 8-anilino 1-naphthalenesulfonic acid (ANS) ammonium salt, was used to obtain the surface hydrophobicity parameters of napin protein, namely the dissociation constant (K_d) and number of ANS binding sites (n-ANS) according to the method of Lamba *et al.*²⁰ with slight modifications. Napin solutions (4 mL) of different concentrations (0.02 - 0.1 mg/mL in 10 mM sodium phosphate buffer, pH 7) were mixed with 20 µL of 8 mM ANS (dissolved in the same buffer as protein) in a vortex mixer for 10 sec and incubated in dark for 15 min. Fluorescence intensities of the resulting solutions were measured using a FluoroMax-4

spectrofluorometer (Horiba Jobin Yvon, Japan) at an excitation and emission wavelengths of 390 and 270 nm, respectively and slit widths of 5 nm. The fluorescence intensity of protein blanks (without ANS) was subtracted from those of the samples to get the net fluorescence intensity. All determinations were carried out in triplicate samples. Values of relative fluorescence (F_R) for each protein concentration was determined using the Equation 1. Surface hydrophobicity index of each napin protein was calculated from the slope of the line generated for napin concentration (mg/mL) vs F_R .

$$\text{Relative fluorescence } (F_R) = (F_p - F_0) / F_0 \quad \text{Equation 1}$$

F_p = Fluorescence intensity of protein-ANS conjugate

F_0 = Fluorescence intensity of aqueous ANS solution

For each ANS-protein interaction, a calibration factor (Q) was determined from the reciprocal plot of $1/F_R$ vs $1/\text{napin concentration}$ as described by Lamba *et al.*²⁰ The plot was extrapolated to infinite protein concentration at $1/[\text{protein}] = 0$ and $1/F_R = 1/F_{R_{\max}}$. The inverse of the Y axis intercept gives the maximum change in F_R ($F_{R_{\max}}$). The calibration factor Q was calculated from Equation 2 in which the $[\text{ANS}]$ is the concentration of ANS at $F_{R_{\max}}$.

$$Q = F_{R_{\max}} / [\text{ANS}] \quad \text{Equation 2}$$

The number of ANS binding sites of each napin protein was obtained from a fixed protein concentration (in the linear range according to the plots for F_R against napin concentration) of 0.1 mg/mL in 10 mM sodium phosphate buffer (pH 7) and 5 to 640 μM ANS (appropriate volumes of ANS solution was added to attain the concentration). The fluorescence intensity of the napin-ANS conjugate was measured as described above. All determinations were done on triplicate samples.

The concentration of ANS bound to proteins (L_B) was determined from relative fluorescence measurement using conversion factor (Q) according to Equation 3.

$$L_B = \frac{F_R}{Q} \quad \text{Equation 3}$$

Scatchard plots for napin-ANS binding were developed as protein bound ANS/ free ANS vs protein bound ANS (L_B/L_F vs L_B). The dissociation constant (K_d) and the number of ANS binding sites were determined from the scatchard equation (Equation 4).

$$\frac{L_B}{L_F} = \frac{nP}{K_d} - \frac{L_B}{K_d} \quad \text{Equation 4}$$

Where, L_B is concentration of ANS bound to protein (μM), L_F is concentration of unbound or free ANS (μM), n is number of ANS binding sites, P is concentration of napin (mg/L), and K_d is the dissociation constant.

Simulated *in vitro* gastrointestinal (GI) digestion of YM

Ground whole seeds of YM+M and YM-M were subjected to simulated GI digestion using a static digestion model as described in Marambe *et al.*²¹ Gastric phase digestion was carried out using porcine pepsin (from porcine gastric mucosa; 2490 units/ mg solid; 3410 units/mg protein) at an enzyme to substrate ratio (E:S, w:w) of 1:250, pH of 2, incubation time of 2 h and temperature of 37 °C. In the intestinal phase digestion, the gastric digest was raised to pH 6.8 and incubated with pancreatin (from porcine pancreas; 8 × USP) at an E:S (w:w) of 1:25 for 4 h at 37 °C. Digested protein samples were obtained at the end of each digestion phase (gastric and gastric + intestinal) and immersed in an ice bath to stop enzyme activity and centrifuged at 8,000×g for 15 minutes. The recovered supernatants of gastric phase (gastric digest; GD) and gastric+intestinal phase (gastric and intestinal digest; GID) were stored in 4 °C and all analyses on digests were conducted within 24 h. Enzyme blanks contained only the digestive enzyme/s without protein and prepared under same conditions. The control samples for gastric phase and gastric+intestinal phase were prepared with protein and simulated digestive fluids without enzymes of the respective digestion phase.

Polypeptide profile analysis

The polypeptide profile of seed, flour, isolated napin, GI digests and residues resulting from digestion of YM were determined using sodium dodecyl sulphate polyacrylamide gel electrophoresis (SDS-PAGE) as described in Wanasundara *et al.*¹⁸ Samples were mixed with β -mercaptoethanol (β -ME) for reducing conditions and β -ME wasn't used for non-reducing conditions. Precast, 8-25 %T gradient gels were used and polypeptide separation, staining and destaining was carried out using PhastSystem electrophoresis system (GE Healthcare). The scanned gel images were analyzed by the Image-Quant[®] software to estimate molecular weight of polypeptide bands and band intensity.

Determination of Sin a 1 AE-Ab reactive napin content

The Sin a 1 AE-Ab reactive napin content of YM+M and YM-M as well as their *in vitro* digests was determined using AE-Ab (raised against the peptide Gln-Gly-Pro-His-Val-Ile-Ser-Arg-Ile-Tyr-Gln-Thr-Ala-Thr having the published amino acid sequence of Sin a 1 epitope)-based NCI-ELISA as described in Marambe *et al.*¹³ The napin protein obtained as described above was reconstituted in borate buffered saline (BSB, pH 8.5) and was used to prepare standards for ELISA (0-27 µg of BSA equivalents/mL). Defatted YM+M and YM-M seeds were extracted with acidified water (pH 3) containing CaCl₂ (0.15 M), diluted with BSB buffer and used to coat 96-micro well plates (100 µL/well). After incubating at 37 °C for 1 h for coating, residual binding sites in the plate and sample were blocked with BSA (1% in BSB) and rabbit polyclonal AE-Ab stock solution (primary ab, 0.9 mg/mL in BSB) diluted with BSB (1: 25,000)) was added to each well (100 µL/well) and incubated at room temperature for 1 h. This was followed by a similar incubation with the secondary Ab, goat anti-rabbit IgG horse raddish peroxidase (HRP) conjugate (diluted to 1: 2000 v/v in BSB; 100 µL/well) and followed by adding, 100 µL TMB (1 mg/mL of methanol) per well for color development. After 20 minutes of TMB addition the color development was arrested by adding 2 M H₂SO₄ (50 µL/well) and the optical density (OD) was read at 450 nm using a microplate reader. The AE-Ab reactive napin content was interpolated from the linear portion of the sigmoidal ELISA standard curve (OD at 450 nm vs napin concentration).

Homology modeling of Sin a 1

The three dimensional structure of Sin a 1 (Accession No: P15322²²; or ALL1_SINAL) was modelled using the SWISS-MODEL²³ (<http://swissmodel.expasy.org>), Swiss PDB viewer²⁴ and PyMOL²⁵ programs. The 3D structure of napin of *Brassica napus* (PDB accession number 1SM7, Solution structure of rPronapin precursor Bn1b) was used as the template. PeptideCutter of the ExPasy server²⁶ was used to predict the theoretical cleavage sites of proteolytic digestive enzymes (pepsin, trypsin and chymotrypsin).

Data analysis

All the standards and samples for ELISA assay were performed replicated four times for each seed sample. The other analyses were carried out in minimum of triplicates. All the values were reported as mean ± standard deviation. Data analysis was performed as a generalized linear

model (one way analysis of variance ANOVA) with mean comparison [Tukey's pair wise comparisons; probability (p) at 0.05] using SAS 9.1 software (SAS Institute Inc., USA).

Results and Discussion

The starting materials used for this study were the whole YM seeds obtained before (YM+M) and after (YM-M) going through industrial myrosinase inactivation process. All YM seed samples were screened for myrosinase activity after receiving according to Palmeiri *et al.*²⁷ The myrosinase activity assessed by using sinigrin as the substrate was reduced by 99 to 100% in YM-M seeds compared to YM+M seeds (results not shown) ensuring the effectiveness of industrial process employed for myrosinase inactivation. The total protein content of the seeds did not change due to this process and recorded a mean value of 32.60% (± 1.18) for YM+M and 32.45% (± 0.16) for YM-M seeds on a dry weight basis. Although these seeds were obtained in random occasions from the processing plant, the protein content varied in a narrow range and fell within the values reported for Canadian YM¹³. According to our previous findings, napin of YM solubilizes completely when pH is 3 and CaCl_2 is present in the solubilizing medium and Sin a 1 constitutes more than 50% of YM napin¹³. Absence of napin related polypeptide bands in the meal residue of both YM+M and YM-M seeds left from pH 3 extraction (Fig. 2A) confirmed complete extraction of napin under the conditions employed. Moreover, the results showed unaltered low pH solubility of napin in YM-M compared to YM+M. Therefore, the napin obtained from pH 3 extraction of these seeds was considered suitable for investigating physico-chemical properties to understand the impact of enzyme inactivation process on the protein structural properties and their ability bind Sin a 1 anti-epitope antibody.

The polypeptide profiles of napin extracts of YM+M and YM-M seeds under non-reducing conditions (Fig. 2B) exhibited the predominant 12.5 kDa band of intact napin. Other than this napin band, several low-intensity bands were observed in the extracts of YM+M (9.7 kDa, 16.0 kDa, 22.8 kDa and 35.6 kDa) and YM-M (9.5 kDa, 15.7 kDa, 16.6 kDa, 23.1 kDa and 28.9 kDa) under non-reducing conditions (Fig. 2B). In napin extracted from YM+M, under the reducing conditions, almost all the minor bands disappeared along with napin band, however, low molecular weight polypeptides and the bands with 10.6 kDa and 8.9 kDa of estimated molecular weights became visible (Fig. 2B). For the napin extracted from YM-M, reducing conditions did

not cause the complete disappearance of minor bands above 12.5 kDa but their intensities were reduced. It could be suggested that the high molecular weight minor polypeptide bands observed under non-reducing condition may be napin aggregates formed while drying. All the napin extracts were lyophilized to obtain a dry protein powder (N-based protein content >99%) and reconstituted in the sample buffer for electrophoresis. Carpenter *et al.*²⁸ have reported protein aggregate formation during lyophilisation. Stable aggregates observed in napin obtained from YM-M seed than YM+M (Fig. 2B) suggested that the enzyme inactivation treatment may have induced some form of napin aggregation.

Impact on structural properties of napin

Secondary structure

The intense positive band at 191 nm and a minimum band at 208 nm and 222 nm (Fig. 3A) in the far UV range (190-260 nm) are typical for α -helix structures and confirmed the predominant helical nature of the napin secondary structure for the proteins obtained from both YM+M and YM-M seeds. The composition of secondary structure components of napin from YM+M and YM-M was not significantly different ($p < 0.05$; Table 1); the α -helical content ranged from 40.3 to 47.5 % and 41.3 to 45.9%, respectively for YM+M and YM-M and was without any detectable difference. These results indicated that the industrial myrosinase inactivation process has not caused any significant changes to the YM napin secondary structure. Sirvent *et al.*²⁹ reported 58-60% α -helix structure for napin of *S. alba*, which is a higher value than the average value of the present study for YM+M napin (43.40%), which could be due to the differences in the medium used for extraction; pyrophosphate buffer at pH 9 vs. pH 3 water containing CaCl_2 and H_2SO_4 (present study) and also the model used for calculation.

Tertiary structure

Analysis of the near UV-CD spectra (260-320 nm) of napin from YM+M and YM-M (Fig. 3B) showed that the peaks at 282 and 292 nms were without any significant change. However the mean residue ellipticity values observed for YM-M were quite low compared to YM+M. The near UV-CD spectra within 250-320 nm arises due to aromatic amino acids (Trp ~290 nm; Tyr 275-282 nm; Phe a weak peak at 255-270 nm) and the tertiary structure foldings of polypeptide chain that lead to arrangement of these side chains in a chiral environment giving rise to near

UV-CD spectra³⁰. Although the reported Sin a 1 allergen sequence²² contains more Phe residues (5 residues) compared to Tyr (1 residue) and Trp (2 residues), both napins analyzed in the current study did not show clear peaks arising due to Phe residues. The near UV-CD spectra of napin of both seed types suggest that myrosinase inactivation treatment may have not induced noticeable changes to napin tertiary structure folds.

Surface hydrophobicity parameters

The binding of fluorescent hydrophobic probe ANS with YM+M and YM-M napin showed a typical hyperbolic response (Fig. 4A) and considerable changes in the binding parameters (dissociation constant; K_d and number of ANS binding sites; n) (Table 1 and Fig. 4B) were identified for YM-M napin. Napin of myrosinase active seed (YM+M) had significantly ($p < 0.05$) higher K_d (94.8 μM) and n (5.65 $\mu\text{moles/mg protein}$) values compared to YM-M napin (K_d of 21.0 μM and n of 1.29 $\mu\text{moles/mg protein}$). The reciprocal of K_d gives the affinity constant, indicating that napin of myrosinase inactivated seed (YM-M) had significantly higher ($p < 0.05$) affinity for ANS than that of YM+M. Moreover, at saturation, YM-M napin required less number of ANS molecules to occupy the available (maximum) binding sites compared to YM+M. Considering the low values resulted in for surface hydrophobicity index (YM-M: 54.66 vs YM+M: 88.05) it is quite possible that the surface hydrophobicity of napin molecules has been altered due to enzyme inactivation process. ANS is essentially non-fluorescent in the aqueous environment and becomes appreciably fluorescent in apolar environments³¹, preferentially binding with the molten globule state of a protein with intact secondary structure and exhibits diminished binding to a fully unfolded protein. The surface hydrophobicity of proteins is also dependent on the amino acid composition and relates to the three dimensional structure and functional properties of protein³². Considering the observations of the current study, it can be predicted that the myrosinase inactivation treatment has caused a reduction in the number of exposed hydrophobic sites on napin surface, therefore low values for surface hydrophobicity index and number of ANS binding sites were reported. The low value for K_d indicates that the remaining hydrophobic sites in the YM-M napin have high affinity towards hydrophobic molecules. Studies on napin and 2S proteins with similar molecular size and rich in internal S-S bonding have reported on reversibility of temperature ($>65^\circ\text{C}$) induced unfolding^{29,33,34}. Although there is no evidence in the present study to suggest that the enzyme

inactivation process caused destruction of napin secondary structure or complete unfolding of the protein, this data sufficiently support possible surface modification leading to certain changes in the molecule surface hydrophobicity. Therefore, we propose a strong possibility of napin protein unfolding at the high temperature of myrosinase inactivation treatment of YM and then refolding upon cooling with alterations in special arrangement of certain side chain amino acid residues residing on the molecule surface.

Binding of Sin a 1 AE-Ab

As described in our previous work¹³ Sin a 1 AE-Ab shows specific binding with napin under non-reducing conditions, particularly with the napin large chain under reducing conditions, when used as the primary Ab in ELISA. According to the present study, YM+M seeds have a Sin a 1 level of 1.05-1.37 g/100 g seeds (16.59-23.16 g/100 g of napin). Interestingly, the enzyme inactivation process has caused a significant increase ($p < 0.05$) in the Sin a 1 AE-Ab binding and resulted in higher Sin a 1 level for the seeds (1.46-2.06 g/100 g of seeds; 36.27-91.07 g/100 g of napin) compared to the same seeds without heat treatment. The level of Sin a 1 of the seeds received for this study was below the range of 2.65 to 5.98 g/100 g of seeds which was reported for commercial varieties produced in Saskatchewan in our previous study and could represent the effect of environmental factors and seed variety.¹³ The increased Sin a 1 level in YM-M compared to YM+M (Table 1) may have caused by the increased accessibility of Sin a 1 epitope to bind with AE-Ab. Although there were no detectable alterations in the tertiary and secondary structure of napin as indicated by structure analysis, one can infer that the increase in AE-Ab reactive napin content shows a possibility of enhanced Sin a 1 allergenic potential of napin protein fraction upon this enzyme inactivation process. Similarly, in a study³⁵ using the major peanut allergen, Ara h 1, the isolated Ara h 1 from roasted peanuts showed enhanced allergenic properties compared to that of unroasted peanuts although the tertiary and secondary structure elements of both proteins were similar. It was suggested that roasting-induced chemical modifications of Ara h 1 molecule surface or degradation of surface glycosylation of Ara h 1 may have exposed the epitopes leading to increased allergenic properties³⁵. In the present study, the increased surface hydrophobicity observed for napin from YM-M seed provides a reliable indication that although remained folded, the heat treatment has enhanced available hydrophobic pockets/patches on the surface of napin than the protein obtained from untreated seed. In

addition, any heat-induced changes that occur in the napin associated molecules may also expose the epitope region leading to an increase in AE-Ab reactivity of YM-M napin.

Simulated gastro-intestinal digestion

Stability of napin and other proteins in YM flour

The polypeptide profiles observed for the soluble fraction of YM+M and YM-M flour at the end of the gastric phase of digestion (Fig. 5A and B) were almost similar. In order to keep the effect of all the seed constituents, the flours of YM were used for simulated GI digestion instead of isolated napin protein. The polypeptide profile of the digests (soluble fraction or supernatant described in methods section) available for YM+M and YM-M at the end of gastric phase and gastric+intestinal phase was monitored to understand the degradation pattern of napin (Fig. 5) with appropriate controls that were kept under same conditions without enzymes. The proteins and protein fragments of the soluble fraction can be considered available to elicit immune responses and the tri and dipeptides and free amino acids can be absorbed. No peptide bands originating from intact cruciferin (11S globulin, 43-55 kDa) were found in the digest and only faint cruciferin bands were found in the residue remaining after gastric phase digestion (Fig. 5C). Therefore it can be assumed that most of the cruciferin protein was degraded due to pepsin activity at pH 2 and 2h of pepsin-assisted hydrolysis. Polypeptide bands originating from napin (~12.5 kDa) were found in the soluble fraction of YM+M and YM-M seeds at the end of gastric digestion phase. The low molecular weight (<10 kDa) fragments of napin observed under NR conditions (Fig. 5A and B) further indicated limited hydrolysis of napin by pepsin during gastric phase digestion similar to the reporting of Sirvent *et al.*²⁹ with purified Sin a 1.

The soluble fraction recovered from the samples after both gastric and intestinal phases of digestion also exhibited polypeptide bands originating from napin but at lower intensity for the YM-M sample than YM+M (Fig 5A and B Lane 5). For example, the napin band of gastric+intestinal digest of YM+M showed only 25% reduction of intensity compared to that of gastric phase, whereas for YM-M there was 77% reduction in intensity. Moreover, a low molecular weight fragment was observed just below the napin band of YM+M. The napin derived <10 kDa fragments found at the end of gastric phase were no longer visible after gastric and intestinal digestion phases indicating further degradation of gastric digested napin and its

fragments during the intestinal phase. Separation of polypeptides under reducing conditions showed that the intensity of napin small chain was particularly reduced for YM-M sample after GI digestion (Fig. 5A Lane 5 vs 6).

According to Mills *et al.*³⁶, an allergen that is sensitized through GI tract is able to preserve its structure from any degradation that occurs during digestion. This allows sufficient amount of allergen to survive in the intact form and taken up by the gut and sensitize intestinal mucosal system. In a review, Moreno *et al.*³⁷ highlighted the importance of combining physiologically relevant *in vitro* simulated GI digestion protocols, taking food matrix into consideration, and in combination with immunological assays to determine the potential allergenicity of an allergen. Upon consumption of YM, napin protein with Sin a 1 isoform get exposed to several proteolytic enzymes in the GI tract that decides the fate of Sin a 1 and how it is presented to the immune system to elicit allergic reactions.

Pepsin, the only proteolytic enzyme found in the gastric phase is an endopeptidase that preferentially hydrolyzes peptide bonds between dicarboxylic amino acids (Glu, Asp) and aromatic amino acids (Phe, Tyr and Trp). Of the pancreatic enzymes, trypsin hydrolyzes the peptide bonds formed by carboxylic groups of Arg and Lys whereas chymotrypsin splits the peptide bonds formed by carboxylic groups of aromatic amino acids³⁸. The pH of the gastric digestion medium was acidic (pH 2) and napin of YM easily solubilizes from the seed matrix at this pH^{13,18}. However, the clear napin band observed in the SDS-PAGE profile of the residue recovered after gastric digestion of both YM+M and YM-M (Fig. 5C) indicates certain amount of napin of YM flours was not solubilized under conditions of gastric phase. This solubility difference may be caused by the high viscous medium created by mucilage and also the interference of oil of YM seed flour. Moreover, 2S albumins are reported to bind or associate with lipids and then show resistance for pepsin digestion³⁹.

Our results showed that napin of both YM+M and YM-M seeds have high degree of resistance to pepsin digestion when incubated for 2h at the gastric pH of 2.0. The resistance for pepsin digestion is used as a marker for assessing potential allergenicity of a protein³⁶. As reported by Astwood *et al.*⁴⁰ the allergenic storage proteins possess digestive stability. According to Fuchs

and Astwood⁴¹, allergens that are less stable in SGF show some stability in SIF. Previously, Astwood *et al.*⁴⁰ showed that complete resistance of Sin a 1 for 60 min digestion in SGF. However, in our study, a significant loss in the intensity of napin protein band was noted after GI digestion of YM-M compared to that of YM+M. According Sirvent *et al.*²⁹ the theoretical cleavage sites (TCS) of Sin a 1 for the pepsin enzyme is mostly located in the protein interior and the number of TCS for the intestinal phase enzymes, trypsin and chymotrypsin are greater than that for pepsin and distributed throughout the three dimensional structure surface of Sin a 1. The TCS modelled on three dimensional structure of Sin a 1 show more trypsin + chymotrypsin cleavage sites on the surface of Sin a 1 compared to that for pepsin (Fig. 6A and 6B). Moreover, our findings on limited hydrolysis in the gastric phase and extensive degradation in the GI phase of Sin a 1-containing napin can validate the explanation that Sirvent and group²⁹ proposed. Furthermore, the myrosinase inactivation process had caused exposure of more cleavage sites of napin molecules for intestinal phase enzymes causing greater degradation of the protein during intestinal phase compared to the untreated. This observation corroborates with the surface modification occurred due to reversible unfolding of napin during heat treatment of myrosinase inactivation of YM seeds.

Sin a 1 AE-Ab reactivity of GI digested YM flour

Gastric phase

At the end of 2h gastric phase incubation, the soluble fraction of YM-M sample had significantly higher ($p<0.05$) levels of AE-Ab reactive napin (1.03 ± 0.02 mg/g of seeds or 2.97 ± 0.06 mg/g of total protein) than the untreated seeds (0.86 ± 0.01 mg/g of seeds or 2.47 ± 0.05 mg/g of total protein) (Fig. 7A). It is clear that more Sin a 1-epitope containing napin has become soluble from myrosinase inactivated seed flour during the acidic pH of gastric phase of digestion. In order to understand whether enzyme activities of the digestive phases caused modifications in the napin molecule's epitope sites or accessibility to AE-Ab, YM flour samples incubated under same conditions without pepsin were investigated. The YM-M showed significantly higher ($p<0.05$) level of AE-Ab reactive napin (1.32 ± 0.05 mg/g of seeds or 3.80 ± 0.15 mg/g of total protein) compared to YM+M (0.92 ± 0.01 mg/g of seeds or 2.64 ± 0.04 mg/g of total protein) in the absence of pepsin, indicating that the myrosinase inactivation process has caused differences in the napin solubility. With the respective proteolytic enzyme in place, both YM+M and YM-M actually

showed a decrease in AE-Ab reactive napin content by 6.5% and 22%, respectively supporting the observation of reduced intensity of polypeptide bands observed in SDS-PAGE profile of gastric digests (Fig. 5A). According to Figure 6A, the linear epitope of Sin a 1 molecule carries one TCS for pepsin. It may be possible that napin of YM-M seeds have this pepsin cleavage site exposed compared to YM+M. Thus release of napin fragments with AE-Ab accessible Sin a 1 epitope sequences and hydrolysis of epitope region by pepsin could be responsible for the observed decrease in AE-Ab reactivity of YM-M napin compared to the control sample. Therefore, it can be considered that myrosinase inactivation process that industry uses does not cause significant elevation in immune reactivity of YM napin.

Gastric and intestinal phase

Upon digestion with pancreatin (pH 6.8) for 4 h after gastric phase, a significant increase ($p < 0.05$) in the AE-Ab reactive napin content in the YM+M (1.81 ± 0.07 mg/g of seeds or 5.17 ± 0.22 mg/g of protein) was observed compared to the samples that were incubated without proteolytic enzymes (1.15 ± 0.03 mg/g of seeds or 3.29 ± 0.06 mg/g of protein). The myrosinase inactivated YM-M had AE-Ab reactive Sin a 1 content of 1.71 ± 0.15 mg/g of seeds or 4.94 ± 0.44 mg/g of protein compared to 2.47 ± 0.38 mg/g of seeds or 7.11 ± 1.09 mg/g of protein resulted in without enzymes, actually a decrease in the reactive protein content (Fig. 7B). When enzyme inactivation process is concerned, slight decrease in the Sin a 1 AE-Ab binding can be seen in the digests of the treated seeds. It is possible that degradation of Sin a 1 napin in YM-M including hydrolysis of Sin a 1 epitope region may have occurred in comparison with YM+M. The SDS-PAGE profile of the digest (Fig. 5A) indicates overall reduction of the intensity for napin including the epitope containing large chain of YM-M seed (Fig 5A, Lane 5). As shown in Fig.6B the Sin a 1 epitope sequence consists of one TCS each for trypsin and chymotrypsin, which are intestinal phase digestive enzyme. Thus, pancreatin activity on YM-M might have increased the accessibility of trypsin and chymotrypsin to the respective TCS in the epitope region causing its hydrolysis and reduction of binding ability with AE-Ab. When AE-Ab binding was compared with seed flours incubated without enzyme, actually the pepsin and pancreatin-assisted hydrolysis did not cause any significant difference in Sin a 1 epitope availability of napin in the YM-M seed than YM+M seeds (Fig. 7A and B).

Pancreatin contains enzymes other than proteases such as lipases and amylases, which may have helped in degrading seed matrix components and enhancing protein exposure and susceptibility for proteolysis in the intestinal phase compared to the gastric phase in which only pepsin is present. Improved protein solubility and facilitation of enzyme accessibility to protein may have caused increase in pancreatin activity on seed components and consequently increasing AE-Ab reactive napin level in GI digested seed samples. However, it should be noted here, that the myrosinase inactivation process resulted in a decrease in the AE-Ab reactive napin content after GI digestion compared to the untreated.

Previous reports show that allergens belonging to 2S proteins are stable for proteolysis^{33,42}. Onaderra *et al.*⁴³ reported that Sin a 1 is highly resistant to trypsin, chymotrypsin and pepsin treatment even after 24 h extensive hydrolysis. In contrast, the current study showed that the hydrolysis of Sin a 1 predominantly by pancreatin during the intestinal phase (4 h) and also more susceptible Sin a 1 is found in YM-M compared to that of YM+M seed. The differences in enzyme to substrate ratios and also the composition of proteolytic enzymes used in these two *in vitro* studies have to be taken into consideration when comparing.

Conclusion

The present investigation shows that the myrosinase inactivation has no major impact on the secondary and tertiary structural features of napin but may cause changes in napin molecule surface leading to altered surface hydrophobicity, susceptibility to digestive enzymes and the allergenic epitope specific antibody binding of the Sin a 1 napin isoform. These process-induced modifications on napin surface may relate to the temperature-induced unfolding and refolding of the molecule. This process enhanced the Sin a 1-containing napin degradation during GI digestion, decreasing its Sin a 1 allergenic epitope specific antibody binding even lower than the seed with myrosinase activity, possibly the alterations occurred in Sin a 1 molecule surface leading to lesser survival of intact epitope during GI digestion.

Acknowledgements

The authors would like to thank Agriculture Agri-Food Canada Risk mitigation Initiative project (RBPI #2105) and Agriculture Development Fund of Saskatchewan Ministry of Agriculture for financial support. Technical support provided by William Hoang is also acknowledged.

Abbreviations

AE-Ab	Anti-epitope antibody
ANS	8-Anilino 1-naphthalenesulfonic acid
BCA	Bicinchoninic acid
BSA	Bovine serum albumin
BSB	Borate buffered saline
CD	Circular dichroism
GI	Gastrointestinal
DSC	Differential scanning calorimetry
p-HBIT	4-Hydroxy benzyl isothiocyanate
NCI-ELISA	Non-competitive indirect enzyme linked immunosorbent assay
YM	Yellow mustard
YM+M	Yellow mustard with active myrosinase
YM-M	Yellow mustard with inactivated myrosinase

References

1. S. Raghavan, in *Handbook of spices, seasonings, and flavorings*, 2nd edn., CRC Press, New York, 2006, ch 5, pp. 63-185.
2. G. R. Fenwick and R. K. Heaney, *Food Chem.*, 1983, **11**, 249-271.
3. W. Cui and N. A. M. Eskin (1998). In *Functional Foods: Biochemical and Processing Aspects*, ed. G. Mazza, Technomic Publishing Company Inc., Lancaster, pp. 235-264.
4. A.M. Nilson and R.A. Holley, *Food Microbiol.*, 2012, **30**, 400-407.
5. S. W. Cui, M. A. Eskin, Y. Wu and S. Ding, *Adv. Colloid Interfac. Sci.*, 2006, **128**, 249-256.
6. X. Wang, D. Wiesenborn, J. Lindley and L. Backer, *T. ASAE*, 1994, **37**, 879-886.
7. Z. O. Saleemi, P. K. J. P. D. Wanasundara and F. Shahidi, *J. Agric. Food Chem.*, 1993, **41**, 641-643.

8. A. Vereda, S. Sirvent, M. Villalba, R. Rodríguez, J. Cuesta-Herranz and O. Palomares, *J. Allergy Clin. Immunol.*, 2011, **127**, 1304-1307.
9. L. Menéndez-arias, I. Moneo, J. Domínguez and R. Rodríguez, *Eur. J. Biochem.*, 1988, **177**, 159-166.
10. M. A. G. Peña, R. I. Monsalve, E. Batanero, M. Villalba and R. Rodríguez, *Eur. J. Biochem.*, 1996, **237**, 827-832.
11. L. Menendez-Arias, J. Dominguez, I. Moneo and R. Rodriguez, *Mol. Immunol.*, 1990, **27**, 143-150.
12. R. I. Monsalve, D. L. P. M. Gonzalez, L. Menendez-Arias, C. Lopez-Otin, M. Villalba and R. Rodriguez, 1993, *Biochem. J.*, **293**, 625-632.
13. H. K. Marambe, T. C. McIntosh, B. Cheng and J. P. Wanasundara, *Food Control*, 2014, **44**, 233-241.
14. A. Spivey, *Environ. Health Persp.*, 2005, **113**, A448.
15. M. Sen, R. Kopper, L. Pons, E. C. Abraham, A. W. Burks, and G. A. Bannon, *J. Immunol.*, 2002, **169**, 882-887.
16. F. J. Moreno and A. Clemente, *Open Biochem. J.*, 2008, **2**, 16-28.
17. AOAC, *Official Methods of Analysis*, Association of Official Agricultural Chemists, Arlington, VA, USA.
18. J. P. Wanasundara, S. J. Abeysekara, T. C. McIntosh and K. C. Falk, *J. Am. Oil Chem. Soc.*, 2012, **89**, 869-881.
19. P. K. Smith, R. I. Krohn, G. T. Hermanson, A. K. Mallia, F. H. Gartner, M. D. Provenzano, E.K. Fujimoto, N.M. Goeke, B. J. Olson and D. C. Klenk, *Anal. Biochem.*, 1985, **150**, 76-85.
20. J. Lamba, S. Paul, V. Hasija, R. Aggarwal and T. K. Chaudhuri, *Biochemistry (Moscow)*, 2009, **74**, 393-398.
21. H. K. Marambe, P. J. Shand and J. P. Wanasundara, *J. Agric. Food. Chem.*, 2011, **59**, 9596-9604.
22. UniProt, <http://www.uniprot.org/uniprot/P15322> (accessed July 2014).
23. Swiss-Model, <http://swissmodel.expasy.org> (accessed July 2014).
24. Swiss-PDB Viewer, <http://spdbv.vital-it.ch/> (accessed July 2014).

25. PyMol <http://www.pymol.org> (accessed December 2013).
26. PeptideCutter-ExPASy http://web.expasy.org/peptide_cutter (accessed July 2014).
27. S. Palmieri, O. Leoni and R. Iori, *Anal. Biochem.*, 1982, **123**,320-324.
28. J. F. Carpenter, M. J. Pikal, B. S. Chang and T. W. Randolph, *Pharm. Res.*, 1997, **14**, 969-975.
29. S. Sirvent, O. Palomares, J. Cuesta-Herranz, M. Villalba and R. Rodríguez, *J. Agric. Food. Chem.*, 2012, **60**, 6011-6018.
30. S. M. Kelly, T. J. Jess and N. C. Price, *Biochim. Biophys. Acta -Proteins and Proteomics*, 2005, **1751**, 119-139.
31. M. Cardamone and N. K. Puri, *Biochem. J.*, 1992, **282**, 589-593.
32. S. Nakai and E. Li-Chan, *Hydrophobic interactions in food systems*. CRC Press Inc., Boca Raton, FL, 1998.
33. S. J. Koppelman, W. F. Nieuwenhuizen, M. Gaspari, L. M. J. Knippels, A. H. Penninks, E. F. Knol, S. L. Hefle, and H. H. J. De Jongh, *J. Agric. Food Chem.*, 2005, **53**, 123-131.
34. T.C. Jyothi, S. Sinha, S.A. Singh, A. Surolia and A.G. Appu Rao, *Biochim. Biophys. Acta*, 2007, **1774**, 907-919.
35. J. B. Nesbit, B. K. Hurlburt, C. H. Schein, H. Cheng, H. Wei and S. J. Maleki, *Mol. Nutr. Food Res.*, 2012, **56**, 1739-1747.
36. E.N.C. Mills, J. Moreno, A. Sancho, J.A. Jenkins and H. J. Wichers, in *Proteins in Food Processing*, Ed. R. Yada , Woodhead Publishing Ltd,Cambridge, UK., 2004, pp. 396–418.
37. F. J. Moreno, *Biomed. Pharmacother.*, 2007, **61**, 50-60.
38. G. P. Talwar and L. M. Srivastava, *Textbook of biochemistry and human biology*. PHI Learning Pvt. Ltd., 2002.
39. G. R. Burnett, M. Wickham, A. Fillery-Travis, J. A. Robertson, P. S. Belton, S. M. Gilbert, A. S. Tatham, P. R. Shewry, and E. N. C. Mills, *Biochem. Soc. Trans.*, 2002, **30**, 916-918.
40. J. D. Astwood, J. N. Leach and R. L. Fuchs, *Nat. Biotechnol.*, 1996, **14**, 1269-1273.
41. R. L. Fuchs and J. D. Astwood, *Food Technol.* 1996, **50**, 83-88.

42. F. J. Moreno, F. A. Mellon, M. S. Wickham, A. R. Bottrill and E. N. Mills, *FEBS J.*, 2005, **272**, 341-352.
43. M. Onaderra, R. I. Monsalve, J. M. Mancheno, M. Villalba, A. M. Pozo, J. G. Gavilanes and R. Rodriguez, *Eur. J. Biochem.*, 1994, **225**, 609-615.

Figure Captions:

Figure 1. Surface diagram (A) and cartoon diagram (B) of Sin a 1 molecule modelled using PyMOL. Napin small chain is depicted in greyish blue, large chain is in violet and the epitope region is in yellow.

Figure 2. Polypeptide profile of YM seed and napin extracted from seed. (A) YM flour (lanes 1 and 3) and residue remained after pH 3 extraction (lanes 2 and 4) obtained from seeds before (YM+M) and after (YM-M) myrosinase inactivation, and (B) napin extracted from defatted meal from same seeds. NR: non-reducing, R: reducing conditions.

Figure 3. Far UV CD spectra (A) and near UV CD spectra (B) of napin protein obtained from YM seed before (YM+M) and after (YM-M) myrosinase inactivation.

Figure 4. ANS binding curve (A) and scatchard plots (B) of napin obtained from YM seeds before (YM+M) and after (YM-M) myrosinase inactivation.

Figure 5. The polypeptide profiles of (A) myrosinase active (YM+M) and (B) myrosinase inactive (YM-M) YM seed flour digests and (C) residue obtained from gastric and gastric+pancreatic phases. Lane 1; ground seed under non-reducing, lane 2; gastric digest under non-reducing, lane 3; gastric digest under reducing, lane 4; gastric+intestinal digest under non-reducing, lane 5; gastric+intestinal digest under reducing, lanes 6 and 9; ground seed, lanes 7 and 10; residues after incubation without pepsin and lanes 8 and 11; residues after gastric digestion with pepsin. Lanes 6 to 11 are under non-reducing conditions.

Figure 6. Surface diagrams of Sin a 1 molecule and the primary structure of Sin a 1 (ALL1_SINAL) marked with potential cleavage sites for (A) pepsin in green, (B) chymotrypsin in black-grey and trypsin in blue. The area occupied by Sin a 1 epitope is shown as sticks in the surface diagrams and in a box in the primary sequence. Grey- blue and violet depicts small and large chains of the molecule, respectively and the 3D models were generated using PyMOL.

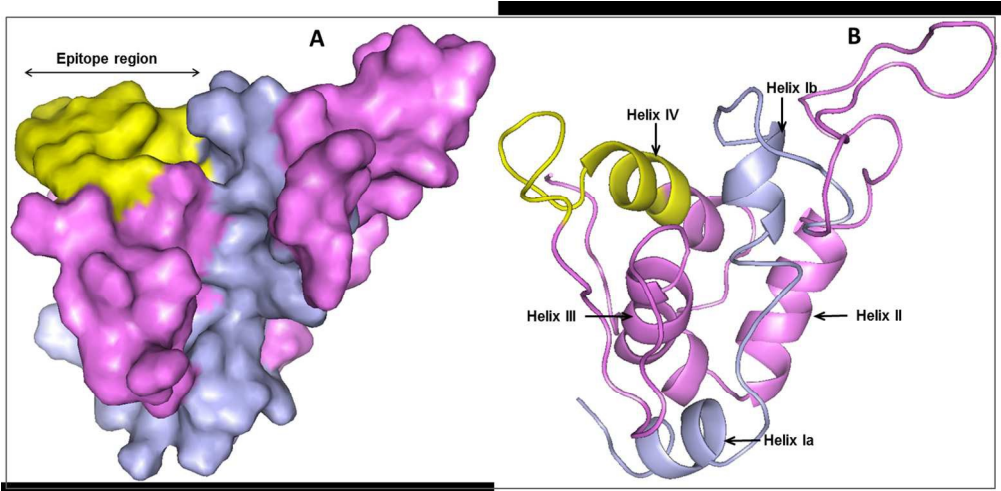
Figure 7. The AE-Ab reactive napin content (mg/g of seeds used) of YM flour at the end of (A) gastric phase and (B) gastric and intestinal phases of digestion. Flour of YM seed before (YM+M) and after (YM-M) myrosinase inactivation was investigated. Control assay mixture was incubated under same conditions without enzymes for the respective digestion phase.

Table 1. Thermal properties, secondary structure components, surface hydrophobicity parameters and Sin a 1 content of napin protein obtained from YM seeds before and after myrosinase inactivation by the industrial process.

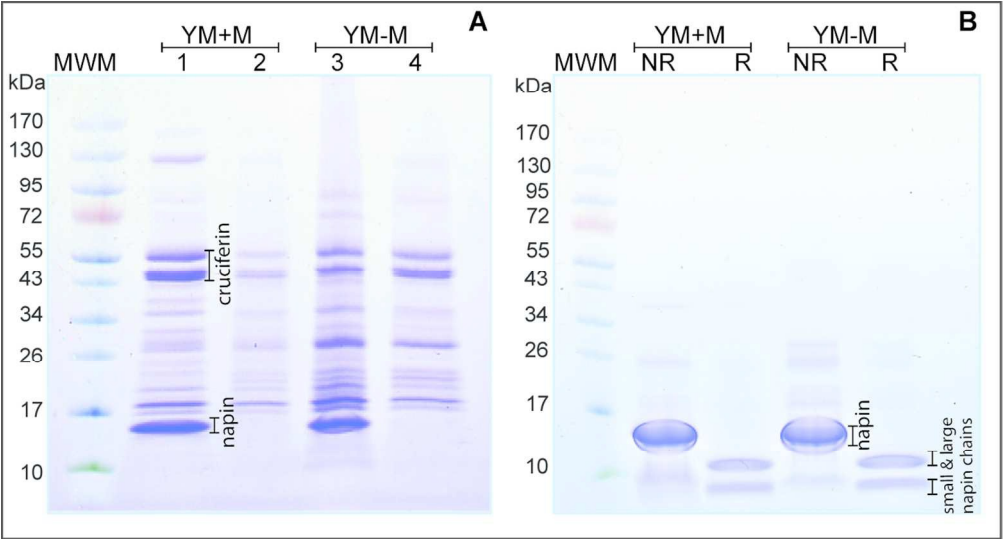
Parameters of napin protein	Myrosinase active (YM+M)	Myrosinase inactivated (YM-M)
Secondary structure components, % ^{1,2} :		
Helix	43.40±3.7 ^a	44.37±2.66 ^a
Antiparallel	6.00±1.21 ^a	6.37±1.33 ^a
Parallel	5.67±0.38 ^a	6.03±0.46 ^a
Beta turn	15.63±2.06 ^a	16.10±2.25 ^a
Random coil	26.40±1.31 ^a	26.60±1.56 ^a
Surface hydrophobicity properties ¹ :		
Dissociation constant (K_d ; μM)	94.80±1.90 ^b	21.05±0.31 ^b
Number of ANS binding sites (n; $\mu\text{moles of ANS/mg of napin}$)	5.65±0.01 ^a	1.29±0.01 ^a
Surface hydrophobicity index (S_0)	88.05±0.88	54.66±0.11
Sin a 1 content ¹ :		
g/100g seeds	1.31±0.08 ^a	1.87±0.26 ^b
g/100 g of pH3 extractable protein (napin)	22.61±1.57 ^a	63.39±4.40 ^b

¹For the given line item mean values in each row with different superscript letters are significantly different ($p < 0.05$)

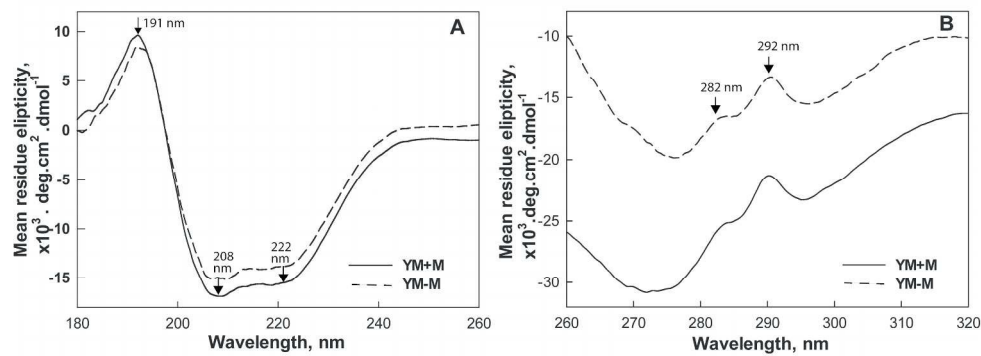
²Values were obtained by analyzing the average ellipticity from CD spectra of samples by CDNN software



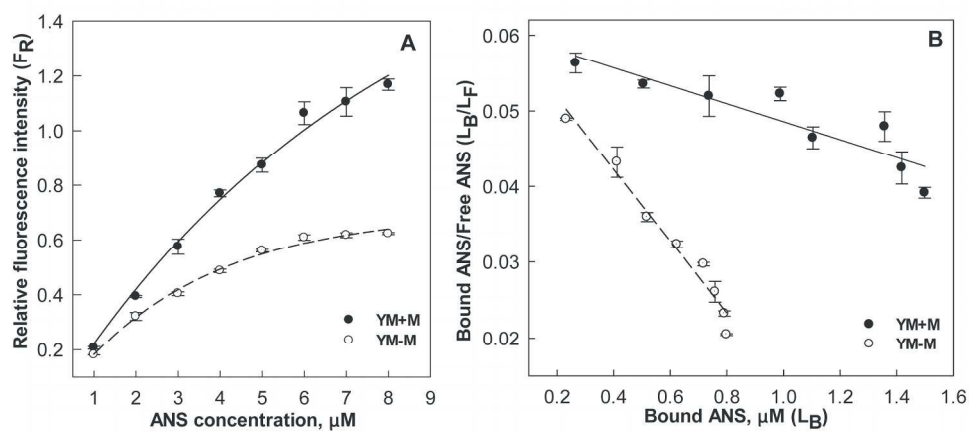
250x122mm (150 x 150 DPI)



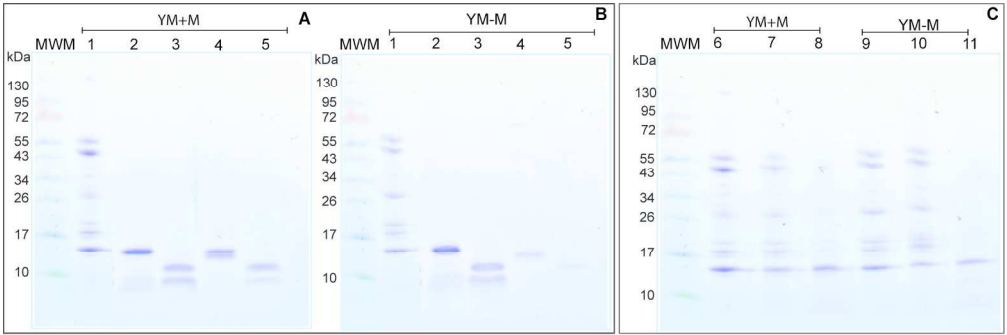
115x62mm (300 x 300 DPI)



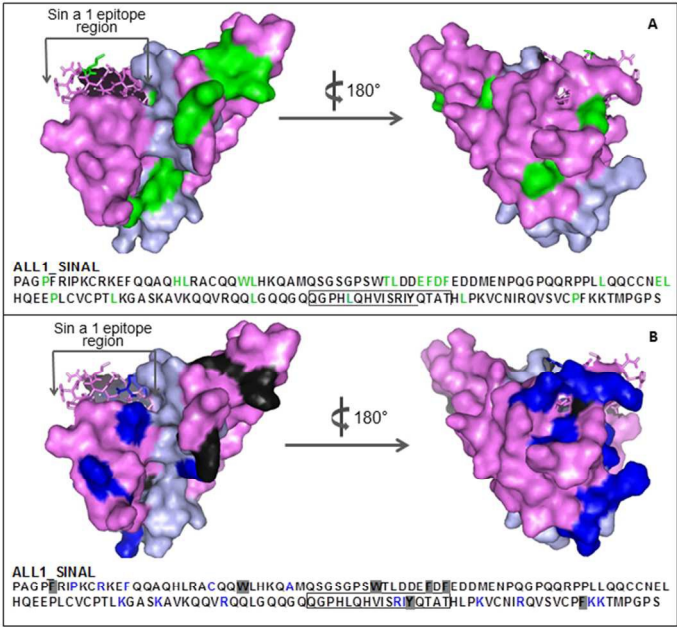
236x93mm (300 x 300 DPI)



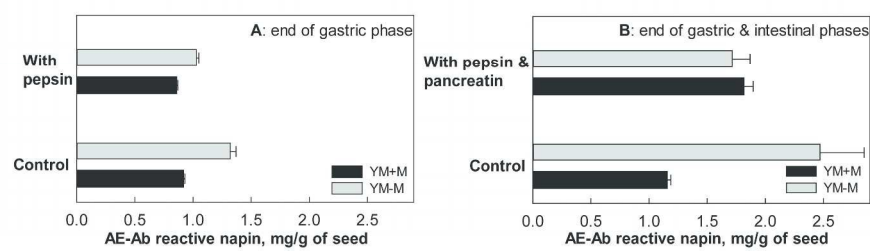
224x127mm (300 x 300 DPI)



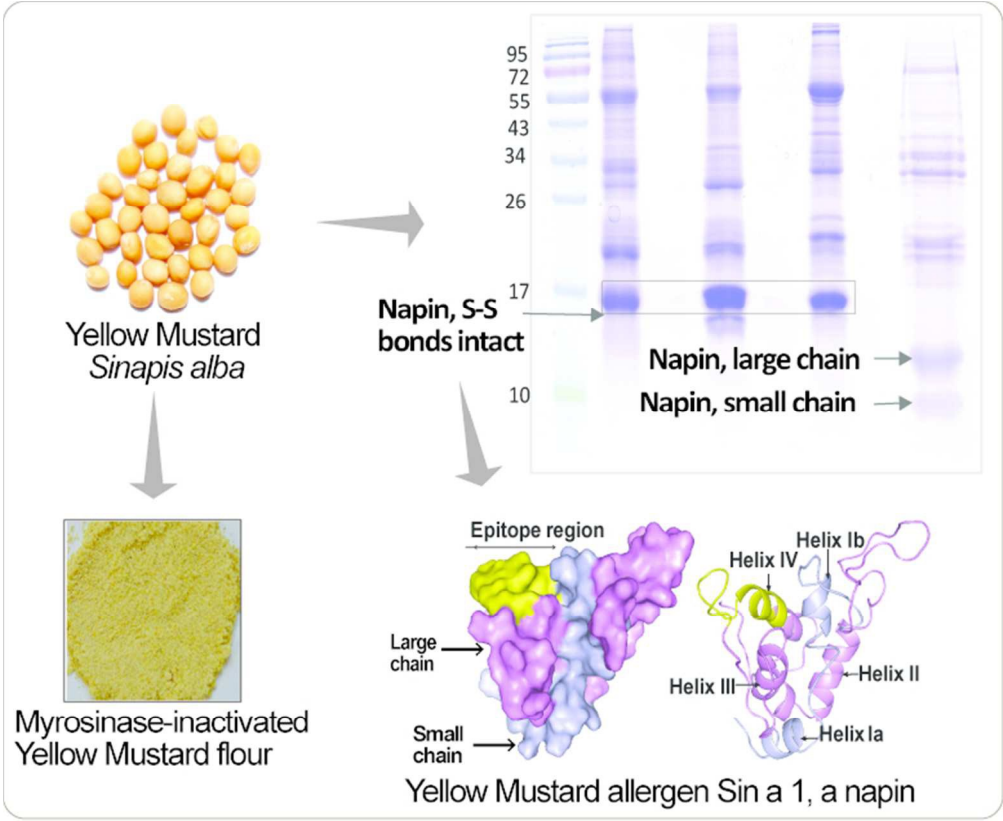
182x60mm (300 x 300 DPI)



254x190mm (96 x 96 DPI)



267x75mm (300 x 300 DPI)



65x53mm (300 x 300 DPI)